2014 5th IEEE RAS & EMBS International Conference on
Biomedical Robotics and Biomechatronics (BioRob)
August 12-15, 2014. São Paulo, Brazil

Robust Torque Control Based on $\mathcal{H}_\infty$ Criterion of an Active Knee Orthosis

Wilian M. dos Santos and Adriano A. G. Siqueira

Abstract— **The authors present in this paper a robust torque control of an active orthosis designed to assist the knee joint flexion/extension during physical therapy. The orthosis is driven by a rotary Series Elastic Actuator presented in authors' previous paper. The adopted control strategy is based on $\mathcal{H}_\infty$ criterion in order to ensure good system performance even when it is subjected to parametric uncertainties and external disturbances. The controller performance is evaluated through the frequency response function analysis. Experimental results involving the interaction between a subject and the active knee orthosis are also presented to show the performance of the developed prototype.**

I. Introduction

To effectively assist human motion and at the same time guarantee patient safety, rehabilitation robots must satisfy certain requirements such as precise and large torque generation, with a bandwidth that approximates the muscular movements one, and the ability to absorb impacts. It is also essential to ensure a backdrivable behavior, characterized by a low mechanical impedance. Traditional stiff and high-precision actuators do not meet these critical requirements [1], [2]. A simple and effective solution, initially proposed in [3], is the SEA concept, where elasticity is intentionally introduced in series between a gear-motor and the load. This configuration allows decoupling the gear-motor inertia and other nonlinearities from the output and isolates the drivetrain from shocks introduced by the load. Another important feature is that the elastic element can be used as a torque sensor considering the linear relationship between spring deflection and torque.

Series Elastic Actuators are able to provide large torque and allow the implementation of torque and impedance control [4], which can be used as a rehabilitation strategy to adjust the level of interaction between device and patient [5]. For example, support torque can be provided by the SEA (properly attached to an orthosis) only when needed during gait training. During the rest of the gait, the SEA should take a low impedance behavior, so that the orthosis is fully complacent with the patient's actions.

A rotary SEA to assist the movement of the lower limbs was presented in [6]. It consists of a geared DC motor, a conventional torsion spring and two rotary potentiometers used to detect the position of the output shaft and the deformation of the spring. In the proposed configuration, the spring is directly placed between the gear-motor and the human joint, therefore supporting large torques. Conventional springs able to support large torques are usually stiff. However, stiff springs deteriorate compliance of the control system, making it difficult to obtain an accurate torque control. Moreover, their nonlinearities are not negligible. Taking into account these considerations, a new rotary SEA model was proposed by the same authors in [7]. In this new configuration, the spring is inserted between the worm gear and the output gears, thereby enabling the use of a spring with lower stiffness. The disadvantage of this configuration is that the nonlinearities associated with the output gears compromises the fidelity of measured torque, increasing the uncertainties in the system.

A solution adopted by some researchers is the development of customized elastic element [8], [9]. In addition to allowing the elastic element to be connected to the load in a direct-drive configuration, this approach can help to overcome some problems like residual deflection, hysteresis and a non-linear behavior in the torque versus angle relationship, that can compromise accurate torque estimation and consequently control performance.

In the authors' previous paper [10], a new rotary SEA, a customized torsion spring, and a conventional control algorithm were presented. However, conventional controllers do not have the capacity to deal with the disturbances caused by interactions with humans. So, in this paper, a control algorithm based on $\mathcal{H}_\infty$ criterion is proposed.

This paper is organized as follows: Section II presents the mechanical design of the rotary SEA and the customized torsion spring; Section III presents the dynamic equation of the system; Section IV presents the robust controller design; Section V presents the results of the implementation of controller and Section VI presents the conclusions.

II. Mechanical Design

In this section, it is presented the design process of the SEA, including the customized torsion spring characterization. The mechanical design was conceived in order to obtain a compact and lightweight architecture. All housing parts were made of aluminium for the purpose of reduced weight. The final assembly of the rotary SEA consists of a) Maxon Motor RE 40, graphite brushes, 150 Watt DC motor, b) worm gear set (M1-150 of HPC Gears International Ltd.) with reduction ratio of 150:1, c) customized torsion spring, d) angular contact bearings, e) magneto-resistant incremental encoder, and f) opto-electronic incremental encoder. The overall dimensions are shown in Fig.1 and the resulting mass

The authors are with the Department of Mechanics Engineering, Engineering School of São Carlos, University of São Paulo, São Carlos, Brazil; Center for Advanced Studies in Rehabilitation, and Center for Robotics of São Carlos. wilianmds@sc.usp.br; siqueira@sc.usp.br

is 2.53 kg, allowing direct mounting of the actuator on the frame of a knee orthosis.

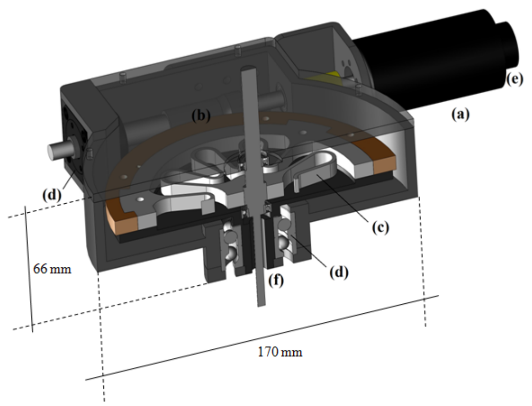

Fig. 1. Cross section of the rotary SEA showing drivetrain components

The design requirements were based on gait pattern data described in [11]. Considering that the maximum power exerted by the knee joint is 0.739 W/kg, with a maximum torque of 0.365 Nm/kg, and that active knee orthosis should be able to supply 60% of the peak torque from the gait pattern of a healthy person with approximately 70 kg, the new robotic device must provide a torque assistance up to than 15 Nm. The minimum torque bandwidth was determined by the Power Spectral Density (PSD) of knee joint torque. Regarding that more than 95% of the PSD of knee joint torque is in the frequency range between 0 and 5 Hz a minimum bandwidth of 5 Hz is defined as a requirement to torque control.

The choice of gear-motor was made based on characteristics of the knee joint considering of gait pattern of a healthy person. The angular velocities of the knee joint are in the range of +/- 50 rpm and the maximum required torque is 15 Nm, while the maximum continuous torque and the maximum speed of the selected motor are respectively 0.181 Nm and 8200 rpm. Therefore a worm gear set with reduction ratio of 150:1 is used to adjust the operating range of motor in order to fulfill the requirements for velocity and torque. Thereby the worm gear output can operate in a velocities range of +/- 55 rpm and, if the efficiency of the gears is not considered, can provide a maximum continuous torque of 27.15 Nm. However, the friction between the gear significantly reduces the efficiency and the torque amplification ratio is not necessarily the same as the ratio speed reduction, [7]. For this reason, a safety factor of 1.8 to the torque requirement is considered.

All relevant information to the control system, i.e. motor rotation, actuator output, and spring deflection estimate, are obtained by two encoders. A magneto-resistant incremental encoder with a resolution of 4096 pulses per revolution in quadrature decoding mode is used to measure the motor rotation and allows to estimate the position of the worm wheel and a opto-electronic incremental encoder with a resolution of 2000 pulses per revolution in quadrature decoding mode is used to measure the actuator output. The spring deflection estimate is obtained by the difference between the position of the worm wheel and the actuator output. The theoretical output torque resolution is given by $k_s(2\pi/2000)$, where k_s is the spring constant.

To meet the requirements of the proposed application the elastic element should be compact, lightweight, and able to withstand high torque with low intrinsic stiffness. However, this characteristics are not found in commercially available torsion springs. For this reason, a new topology torsion spring was developed. Fig. 2(a) shows perspective view of the torsion spring. It is composed of two rings interconnected by flexible elements. The shape and size of the flexible elements were defined by finite element analysis, see [10] for details. The material selected for analysis and fabrication was chromium-vanadium steel (AISI 6150), with a Young's modulus of 205 GPa and a yield strength of about 1320 MPa after a heat treatment process. The torsion spring has been manufactured using the Wire Electrical Discharge Machining (WEDM) process. The mass of the spring is 0.384 kg with a thickness of 8 mm and maximum diameter of 125 mm. The final assembly of the rotary SEA is shown in Fig. 2(b).

(a) Customized torsion spring (b) Rotary Series Elastic Actuator

Fig. 2. Picture of the developed prototype

Fig. 3 shows a preliminary setup of a knee orthosis with the rotary SEA attached to it.

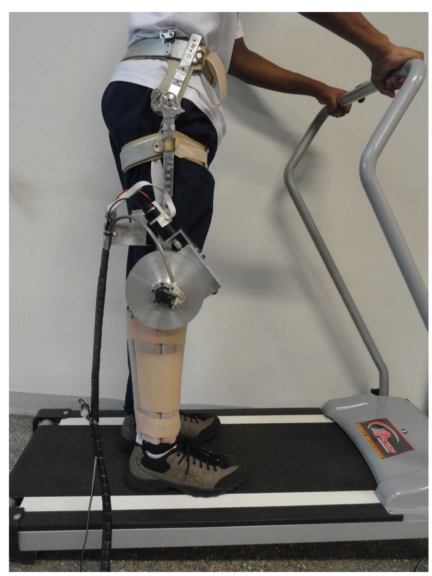

Fig. 3. Rotary SEA attached to a knee orthosis

III. Dynamic Model of the System

The dynamic equation of the rotary SEA can be obtained by applying Newton's Laws, as described in the sequence.

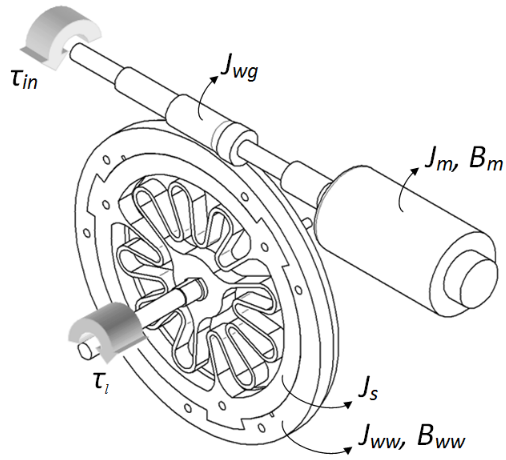

Fig. 4. Dynamic model of the rotary SEA

The input torque (τ_{in}) can be expressed by

$$\tau_{in} = \tau_m - (J_m + J_{wg})\ddot{\theta}_m - B_m\dot{\theta}_m, \tag{1}$$

where τ_m represents the torque generated by the motor, J_m and J_{wg} the inertias of the motor and the worm gear, respectively, and B_m the damping coefficient of the motor.

Similarly, the output torque (τ_{out}) can be written as

$$\tau_{out} = (J_s + J_{ww})\ddot{\theta}_{ww} + (B_{ww})\dot{\theta}_{ww} + \tau_l, \tag{2}$$

where J_s and J_{ww} represent, respectively, the inertias of the spring and worm wheel, B_{ww} the damping coefficient of the drivetrain, and τ_l the torque applied to the load that can be calculated as $\tau_l = k_s(\theta_{ww} - \theta_l)$, where k_s is the spring constant.

Since the torque generated by the motor is amplified by the speed reduction ratio, the following kinematic conditions can be considered

$$\tau_{out} = N\tau_{in} \tag{3}$$

and

$$\dot{\theta}_{ww} = N^{(-1)}\dot{\theta}_m, \tag{4}$$

where $N^{(-1)}$ is the reduction ratio.

Substituting (1) and (2) into (3), and (4) into the resulting equation, one obtains

$$J_{eq}\ddot{\theta}_{ww} + B_{eq}\dot{\theta}_{ww} = N\tau_m - \tau_l, \tag{5}$$

being J_{eq} the equivalent inertia and B_{eq} the equivalent damping coefficient, defined as

$$J_{eq} = J_{ww} + J_s + (J_m + J_{wg})N^2, \tag{6}$$

$$B_{eq} = B_{ww} + (B_m)N^2. \tag{7}$$

In the adopted approach, the motor is treated as a velocity source. According to [12], [13] this approach helps to overcome some undesirable effects of the gear-motor such as static and dynamic friction intrinsic to the drivetrain. Therefore, considering that the desired current is equal to the actual current, the motor torque (τ_m) can be calculated as

$$\tau_m = k_t(k_p(\dot{\theta}_m^d - \dot{\theta}_m) + k_i\int_0^t(\dot{\theta}_m^d - \dot{\theta}_m)dt), \tag{8}$$

where k_p and k_i are the proportional and integral gains of the velocity controller and k_t the torque constant of the motor.

Rewriting (4), the following relation can be obtained

$$\theta_{ww} = \frac{1}{N}\int_0^t(\dot{\theta}_m)dt. \tag{9}$$

Consider the change of variable, where $\dot{\theta}_m$ is replaced by ω_m and substituting (8) and (9) into (5), taking the Laplace transform of equations, one gets the open-loop transfer function of the system as a function of two variables θ_{ww} and ω_m. However, for the controller design consider the case where the load is fixed (θ_l = 0). Therefore, open-loop transfer function of the system is given by

$$\frac{\tau_l(s)}{\omega_m(s)} = \frac{(\frac{Nk_sk_tk_p}{J_{eq}})s + (\frac{Nk_sk_tk_i}{J_{eq}})}{s^3 + (\frac{B_{eq}+k_pN^2}{J_{eq}})s^2 + (\frac{k_s+k_iN^2}{J_{eq}})s}, \tag{10}$$

where the parameters of the equation are defined in Tab. I.

TABLE I

Rotary Series Elastic Actuator Parameters

J_{eq} (kgm^2)	B_{eq} (Nms/rad)	k_t (A/Nm)	k_s (Nm/rad)	N no unit	k_p (Nms/rad)	k_i (Nm/rad)
0,47	60	0,03	105	150	11,9	1,19

The parametric uncertainties and external disturbances acting on the plant input can be grouped in a combined disturbance $w(t)$. The state space representation of rotary SEA, regarding the above assumptions, can be computed as

$$\begin{aligned}\dot{x}(t) &= Ax(t) + B_1u(t) + B_2w(t) \\ y(t) &= Cx(t) + Du(t)\end{aligned} \tag{11}$$

where $x(t)$ is the state, $y(t)$ the measured output, $u(t)$ the control input, and

$$A = \begin{bmatrix} \frac{B_{eq}+k_pN^2}{J_{eq}} & \frac{k_s+k_iN^2}{J_{eq}} & 0 \\ I & 0 & 0 \\ 0 & I & 0 \end{bmatrix}, \quad B_1 = B_2 = \begin{bmatrix} 1 \\ 0 \\ 0 \end{bmatrix},$$

$$C = \begin{bmatrix} 0 & \frac{Nk_sk_tk_p}{J_{eq}} & \frac{Nk_sk_tk_i}{J_{eq}} \end{bmatrix}, \quad D = \begin{bmatrix} 0 \end{bmatrix}.$$

IV. Robust Controller Design

In this section are presented the basics of linear $\mathcal{H}_\infty$ control design and the procedures to apply it for torque control of rotary SEA. The reader is referred to the vast literature on the subject for more details in [14]. Fig. 5 shows the system block diagram, where $P(s)$ represents the plant and $K(s)$ the controller. The plant has two sets of input signals, the internal input u and the external input w, and two sets of output signals, the measured signal y and the regulated output z.

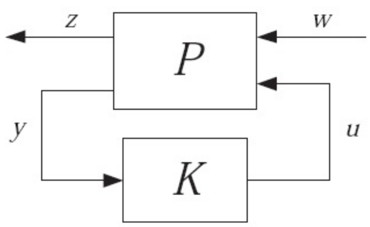

Fig. 5. Block diagram for $\mathcal{H}_\infty$ control systems

The objective of an $\mathcal{H}_\infty$ controller is to guarantee that the $\mathcal{H}_\infty$ norm of a multivariable transfer function $T_{zw}(s)$ is bounded by a level of attenuation γ, $\|T_{zw}(s)\|_\infty < \gamma$. The parameter γ indicates the level of robustness of the control system, or how much the input disturbances are attenuated in the output of the system.

The design of the robust controller is performed considering the nominal model and weighting functions specially selected to improve controller performance. Started by finding a state-space realization of the augmented plant $P(s)$ through the definition of the performance objectives $W_e(s)$ and $W_u(s)$, which are related to the frequency response of the sensitivity function $S(s) = (I + P(s)K(s))^{-1}$, where $K(s)$ is the robust controller. To define $W_e(s)$, we select a bandwidth ω_b, a maximum peak M_s, and a small $\epsilon > 0$. With these specifications in hand, the following performance-shaping, diagonal weighting matrix can be determined as

$$W_e(s) = \frac{s + \omega_b}{M_s(s + \omega_b \epsilon)}. \tag{12}$$

To define $W_u(s)$, we select the maximum gain M_u of $K(s)S(s)$, the controller bandwidth ω_{bc} and a small $\epsilon_1 > 0$ such that

$$W_u(s) = \frac{s + \omega_{bc}}{M_u(\epsilon_1 s + \omega_{bc})}. \tag{13}$$

In the $\mathcal{H}_\infty$ design procedure, they are selected in order to guarantee

$$||S(s)||_\infty \leq ||W_e^{-1}(s)||_\infty$$

and

$$||K(s)S(s)||_\infty \leq ||W_u^{-1}(s)||_\infty$$

The $\mathcal{H}_\infty$ torque control was designed considering the weighting functions parameters shown in Tab. II.

TABLE II
Weighting Functions Parameters

M_s (dB)	ω_b (rad/s)	ε	M_u (dB)	ω_{bc} (rad/s)	ε_1
764	600	0.0012	$5.62 \cdot 10^5$	10^3	0.01

From (12) and (13), and procedures described previously, the following controller K(s) is achieved

$$K(s) = \frac{4420s^2 + 4.42 \cdot 10^8 s + 3.7 \cdot 10^8}{s^3 + 1920s^2 + 1.34 \cdot 10^6 s + 9.373 \cdot 10^5}. \tag{14}$$

Fig. 6 shows the graphics of the sensitivity function $S(s)$ versus the weighting function $W_e^{-1}(s)$, and of $K(s)S(s)$ versus $W_u^{-1}(s)$ for the resulting controller. Note that the controlled plant curves are lower than the weighting functions for all frequency.

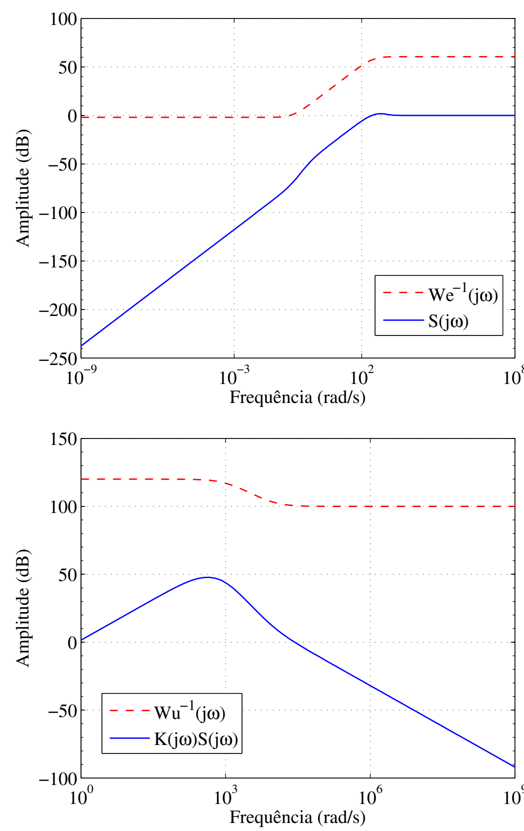

Fig. 6. Sensitivity function $S(s)$ vs. $W_e^{-1}(s)$ and $K(s)S(s)$ vs. $W_u^{-1}(s)$

V. Implementation and Experiments

The control hardware consists of a EPOS 24/5 Positioning Controller sold by Maxon Motor and an ordinary computer hardware equipped with a CAN communication card sold by National Instruments. The EPOS is a full digital smart motion controller capable of operating in position, velocity and current modes. The device also is responsible to decode the signals from quadrature encoders. The communication interface between the computer hardware and the EPOS controller is performed by CANopen communication protocol. The frequency of the control-loop is set at 200 Hz.

The block diagram of the torque control loop is illustrated in Fig. 7. The inner velocity loop was performed by the built-in EPOS velocity control and the controller parameters were automatically determined by the device. The torque controller and metrics considered to measure their performance were implemented through the programming interface Microsoft Visual Studio in the computer hardware, as described in sequence.

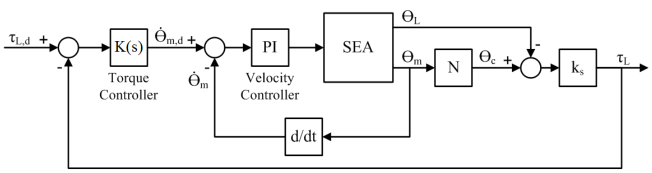

Fig. 7. Robust torque controller with inner velocity loop

A. Torque control bandwidth

Torque control bandwidth of the SEA was evaluated through the frequency response function (FRF) analysis proposed in [15]. To implement the estimation method, the desired torque ($\tau_{l,d}$), seen here as input signal, was defined as a chirp signal with amplitude of 5 Nm and frequency varying from 0 to 20 Hz and back to 0 Hz in over a period of 20 s. The signal is repeated four times, totaling a sampling period of 80 s. Fig. 8 shows the Bode plot of the closed loop transfer function computed from $H_1(\omega)$ and $H_2(\omega)$ estimators and the coherence function $C(\omega)$. From the bode plot, the torque control bandwidth is approximately 9.6 Hz.

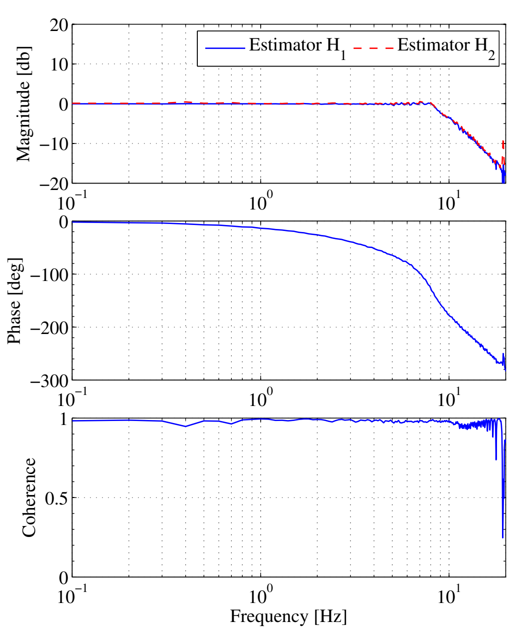

Fig. 8. Toque control response frequency

B. Experimental results with active knee orthosis

According to [6], to realize a good torque control in robots interacting with humans, an accurate actuation system with low impedance is desired. In other words, the active orthosis must follow the knee joint motion, so that the subject does not feel any resistance, when the desired torque is zero. Therefore, the following experiment was performed. One subject walked on a treadmill using the active knee orthosis with the desired torque set to zero.

As expected, the motor followed the human joint motion to keep zero spring deflection. Fig. 9 shows the angle and velocity of the knee joint and the interaction torque between user's limb and the active orthosis, for a gait cycle duration of 3 s. Note that the resistive torque generated by the actuator is proportional to the joint angular velocity. This is due to the presence of an intrinsic damping in the actuator [16]. That is, the active knee orthosis works like a damper, when the desired torque is set to zero. Note also that the stability was not affected by the human motions.

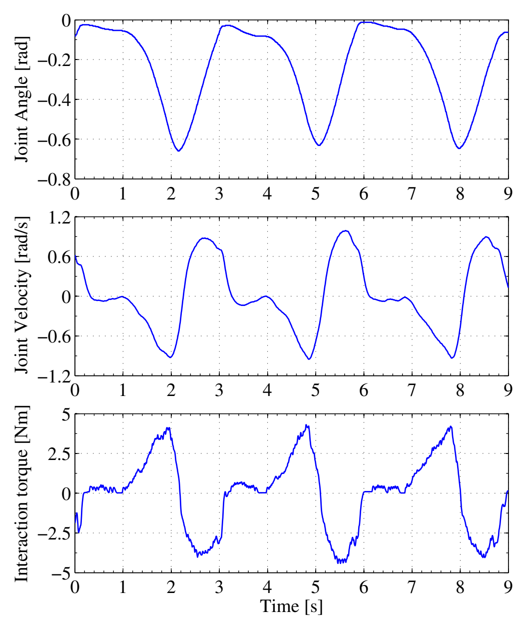

Fig. 9. Experimental data of active orthosis during walking when the desired torque is set to zero

The active knee orthosis was commanded to track a torque profile defined as a sine wave with amplitude of 6 Nm and frequency of 0.1 Hz, in order to evaluate accuracy and robustness of the adopted control strategy while interacting with a human. Fig. 10(a) shows the reference and actual torque as well as magnitude of the torque error when the subject resisted the generated torque, i.e., the knee joint angle is zero. The root mean square (rms) value of the torque error is 0.1 Nm, demonstrating that the active orthosis is able to generate the desired torque accurately. Fig. 10(b) shows the knee joint angle, the reference and actual torque and magnitude of the torque error when the subject is complacent with the generated torque. The rms value of the torque error is 1.06 Nm. Note that the torque error shown in Fig. 10(b) is much greater than that shown in Fig. 10(a) because the human motion. However, it should be noted that the stability was not affected.

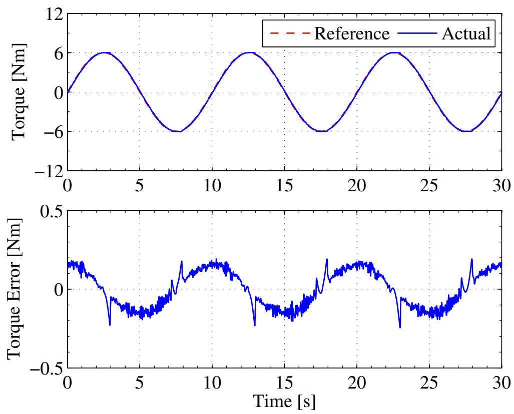

(a) with movement restriction

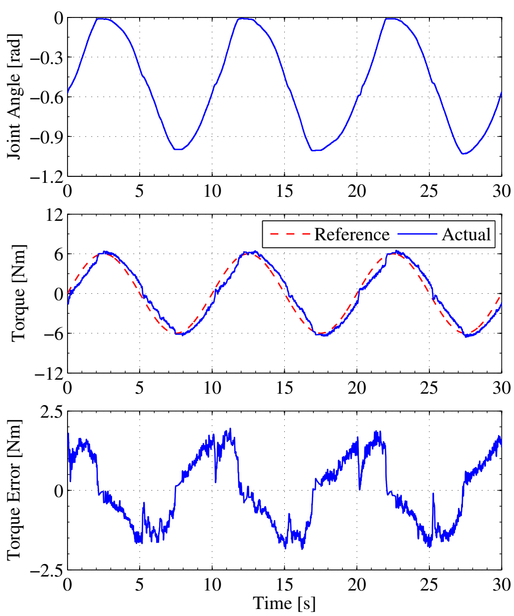

(b) without movement restriction

Fig. 10. Experimental data of active orthosis when the desired torque is set as a sinusoidal wave

VI. Conclusion

This paper presented a robust torque control of an active orthosis designed to assist the knee joint flexion/extension during physical therapy. The performance of the controller was evaluated through the frequency response function analysis. The adopted control strategy, based on $\mathcal{H}_\infty$ criterion, allows the rotary SEA to provide a continuous torque of 5 Nm with a bandwidth of 9.6 Hz. Experiments, involving the interaction between a subject and active orthosis, were performed in order to evaluate performance of the developed prototype. The initial results show that the proposed control method has good performance with respect to external disturbances.

Acknowledgment

This work was supported by São Paulo Research Foundation (FAPESP) under grant n^o 2011/04074-3.

References

[1] A. D. Santis, B. Siciliano, A. D. Luca, and A. Bicchi, "An atlas of physical human robot interaction," *Mechanism and Machine Theory*, vol. 43, no. 3, pp. 253–270, 2008.

[2] R. V. Ham, T. G. Sugar, B. Vanderborght, K. W. Hollander, and D. Lefeber, "Compliant actuator designs," *Robotics Automation Magazine, IEEE*, vol. 16, no. 3, pp. 81–94, 2009.

[3] G. Pratt and M. Williamson, "Series elastic actuators," in *Proceedings of the 1995 IEEE/RSJ International Conference on Intelligent Robots and Systems*, vol. 1, Pittsburgh, USA, 1995, pp. 399–406.

[4] N. Hogan, "Impedance control: an approach to manipulation," *Journal of Dynamic Systems Measure Control*, vol. 107 (Parts 1-3), no. 1, pp. 1–24, 1985.

[5] F. Sergi, D. Accoto, G. Carpino, N. L. Tagliamonte, and E. Guglielmelli, "Design and characterization of a compact rotary series elastic actuator for knee assistance during overground walking," in *The Fourth IEEE RAS/EMBS International Conference on Biomedical Robotics and Biomechatronics*, Roma, Italy, 2012, pp. 1931–1936.

[6] K. Kong, J. Bae, and M. Tomizuka, "Control of rotary series elastic actuator for ideal force mode actuation in human robot interaction applications," *IEEE/ASME Transactions on Mechatronics*, vol. 14, no. 1, pp. 105–118, 2009.

[7] ——, "A compact rotary series elastic actuator for human assistive systems," *IEEE/ASME Transactions on Mechatronics*, vol. 17, no. 2, pp. 288–297, 2012.

[8] C. Lagoda, A. Schouten, A. Stienen, E. Hekman, and H. van der Kooij, "Design of an electric series elastic actuated joint for robotic gait rehabilitation training," in *Proceedings of 3rd IEEE RAS and EMBS International Conference on Biomedical Robotics and Biomechatronics*, Tokyo, Japan, 2010, pp. 21–26.

[9] G. Carpino, D. Accoto, F. Sergi, N. L. Tagliamonte, and E. Guglielmelli, "A novel compact torsional spring for series elastic actuators for assistive wearable robots," *Journal of Mechanical Design*, vol. 134, no. 12, pp. 1–10, 2012.

[10] W. M. Santos, G. A. P. Caurin, and A. A. G. Siqueira, "Torque control characterization of a rotary series elastic actuator for knee rehabilitation," in *16th International Conference on Advanced Robotics*, Montevideo, 2013.

[11] C. Kirtley, *Clinical Gait Analysis: Theory and Practice*, 1st ed. Elsevier Churchill Livingstone, 2006.

[12] D. W. Robinson, "Design and analysis of series elasticity in closed-loop actuator force control," Ph.D. dissertation, Massachusetts Institute of Technology, Cambridge, 2000.

[13] G. Wyeth, "Control issues for velocity sourced series elastic actuators," in *Proceedings of the Australasian Conference on Robotics and Automation*, Auckland, New Zealand, 2006, pp. 1–6.

[14] A. A. G. Siqueira, M. H. Terra, and M. Bergerman, *Robust Control of Robots: Fault Tolerant Approaches*. London: Springer, 2011.

[15] N. M. M. Maia and J. M. M. Silva, *Theoretical and Experimental Modal Analysis*, ser. Engineering dynamics series. Research Studies Press Limited, 1997.

[16] W. M. Santos and A. A. G. Siqueira, "Impedance control of a rotary series elastic actuator for knee rehabilitation," in *19th World Congress of the International Federation of Automatic Control*, Cape Town, South Africa, 2014, to be published.